БЪЛГАРСКА АКАДЕМИЯ НА НАУКИТЕ. BULGARIAN ACADEMY OF SCIENCES

ГЕОХИМИЯ, МИНЕРАЛОГИЯ И ПЕТРОЛОГИЯ. 30. София. 1995
GEOCHEMISTRY, MINERALOGY AND PETROLOGY. 30. Sofia. 1995

Kinetically induced morphological changes in laboratory-grown wulfenite crystals

Ilia Vesselinov

Веселинов, И. 1995. Морфоложки изменения на изкуствени вулфенитови кристали, предизвикани от кинетични фактори. — *Геохим., минерал. и петрол.*, **30**.

Публикуваните данни върху лабораторната кристализация на вулфенита в условия, близки до природните, сочат, че морфологията на кристалите му се влияе силно от кинетични фактори, свързани с химичния състав на средата. Минералът е получаван от азотнокисели водни разтвори при стайна температура и атмосферно налягане чрез реакция на оловни и молибдатни йони. Кристалите му, със средни размери около половин милиметър, са с хабитусни форми *c* {001}, *e* {112}, *n* {011} и (χ) {211} (или {121}) в различни комбинации. Те са изследвани с отражателна гониометрия, сканираща електронна микроскопия, химично разяждане и компютърно чертане. Изкуственият вулфенит има осно отношение $c:a=2{,}233\pm0{,}013$, определено чрез гониометрия на 32 кристала. Не са наблюдавани сигурни случаи на полярно развитие, хемиморфия. Хабитусът на вулфенита е много чувствителен към отношението на концентрациите на реагентите в разтвора около растящите кристали. При $Pb:MoO_4>1$ той е бипирамидален, *e* или *e*+*n*, и стръмно бипирамидален, (χ) или (χ)+*e*. При обратни отношения кристалите растат като плочки с различна дебелина, развивайки пинакоида *c*. Концентрацията на азотната киселина влияе върху характера на кристалните повърхности и върху остеняването. За формите на растеж при по-ниски концентрации, $pH\sim2{,}0\div1{,}5$, са характерни *e*, *n* и *c* с гладки и плоски стени, наречени „плоскостени“. При по-високи концентрации, $pH\sim1{,}5\div1{,}3$, в остеняването преобладават (χ), *c* и по-рядко *n* с гладки, но криви, изпъкнали стени, наречени „кривостени“. Показано е, че тези резултати биха могли да обяснят подобни морфоложки явления при естествения вулфенит. Като вероятен механизъм, забавящ растежа на хабитусните кристални повърхности, е предложена избирателната адсорбция на определени йони. Сходен модел може да обясни полярността на вулфенита като хипоморфизъм, свързан с растежа му, при който взаимодействието кристал-среда се подчинява на закона на Кюри.

Ключови думи: вулфенит, шеелити, кристализация от разтвори, форми на растеж, полярни кристали, хипоморфизъм, избирателна адсорбция.

Адрес: Българска академия на науките, Геологически институт, 1113 София.

Introduction

The long history of morphological studies on wulfenite has raised a number of challenging questions about the growth factors which control the habit modification and face development of thattypical supergene mineral. In the early sixties three important works of Kostov (Костов, 1961; Костов,

1962; Kostov, 1965) put the available evidence into the general context of his genetic scheme of habit types which had introduced the concepts of geno- and phenotypes in mineralogy. In it, the morphology of mineral crystals in general, and of wulfenite in particular, was systematically treated as controlled by static (structural) and dynamic (environmental) factors (Костов, 1973; 1993). Since then voluminous new evidence on wulfenite and related natural and artificial phases has accumulated. This study is an attempt to organize part of it in Kostov's systematic manner in order to throw light on morphological phenomena which may help to judge about some environmental factors in wulfenite growth. They concern the two contrasting habits of the mineral, tabular and dipyramidal, that occasionally occur together even in a single hand specimen, and the steep-dipyramidal crystals of convex faces found in some localities (e. g. Grafenauer, Mirtič, 1972,; Zirkl, 1988; Hanneberg, 1889; Mineralogical Record, 1990; Rothwell, Mason, 1991; Костов, 1993). The arguments here are based on observations and measurements of crystals grown in the laboratory mostly by the author. For reasons which will become clear in the discussion, wulfenite is treated as tetragonal-dipyramidal, *4/m* (sp. gr. C_{4h}^6-$I4_1/a$, Leciejewicz, 1965), rather than pyramidal, *4*, as accepted in mineralogy (Костов, 1993).

Growth experiments

In the laboratory, lead molybdate has been grown from fluxes, hydrothermally and from the melt (e. g. Gmelin, 1976; Mineralogical Record, 1990) but its formation in nature is best reproduced by the methods of chemical reactions in aqueous solutions (Kirov, 1972; Vesselinov, 1976a) which permit to grow crystals at atmospheric pressure and ambient temperature, i. e. under conditions similar to those in an oxidation zone. Such experiments, carried out in the seventies (Kirov, 1972; Vesselinov, 1976a, 1977; Pillai, Ittyachen, 1977a, b), produced crystals of the strikingly varied morphology so typical of the mineral although they were obtained in acid solutions, pH 6 to 1, whereas natural wulfenite is commonly formed in alkaline environments (Кольковски, Бресковска, 1965; Kol'kovski, Breskovska, 1968). The most pronounced morphological phenomena observed will be described below in the light of earlier studies of the author (Vesselinov, 1980; Веселинов, 1992).

The crystals, grown by counterdiffusion of sodium or ammonium molybdate and lead nitrate in silicagel (Vesselinov, 1977) and free of gel systems (Kirov, 1972) acidified by nitric acid to various pH, reached 0,5 mm in size and exhibited *c* {001}, *e* {112} and *n* {011} as habit forms. In both types of systems, dipyramidal *e* or *e*+*n* combinations were formed near the lead reservoirs, whereas close to the molybdate reservoirs the crystals developed more or less pronounced pinacoids. Similar separation of habits in the growth systems had already been observed in calcite (Kirov et al., 1972). In the case of wulfenite, however, the phenomenon was accompanied by colour variations because the molybdate solution reacted with the silica from the gel to produce soluble silicomolybdic acid of lemon-yellow colour which was taken up by the crystals at the molybdate side of the systems so that the platelets were yellow whereas the dipyramids on the lead side were colourless (Vesselinov, 1977), as shown in Fig. 1. Thus, conclusive evidence was gained demonstrating the morphological effect, of solution chemistry which,

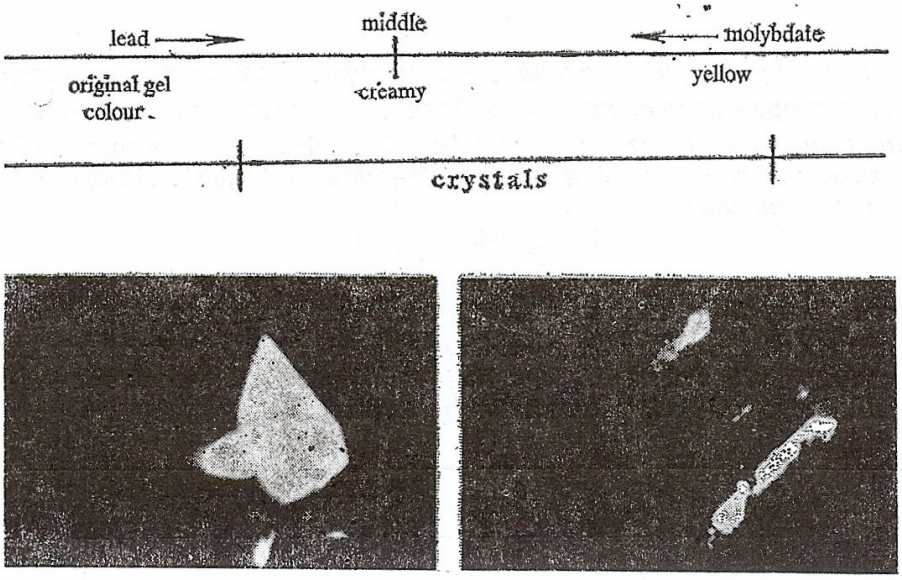

Fig. 1. Colour pattern in the wulfenite gel-growth systems (V e s s e l i n o v, 1977) and the related habits: tabular *c* crystals with minor *e* on the molybdate side, and dipyramidal *e* crystals with minor *n* on the lead side

Фиг. 1. Изменение на цвета в опитите за кристализация на вулфенит в силикагел (V e s s e l i n o v. 1977) и съответните хабитуси: жълти плочести *c* кристали с малка *e* откъм молибдатната страна и безцветни бипирамидални *e* кристали с малка *n* откъм оловната страна

like in the case of calcite (K i r o v et al., 1972), was attributed to the excess of molybdate, resp. lead ions in the solution around the growing crystals (V e s s e l i n o v, 1980; В е с е л и н о в, 1992). P i l l a i, I t t y a c h e n (1977a, b) obtained similar results in silicagel systems; they did not report any colouration of solutions, yet in their analysis, based on the work of K i r o v (1972), they had also reached the conclusion that the habit-modifying factor was the excess of molybdate or lead ions in solution, along with the pH.

The counterdiffusion systems, however, did not permit direct control over the reaction and growth conditions in the crystallization space. A continuous-flow system was constructed (V e s s e l i n o v, 1976a) with which direct evidence was gained on the effect of stoichiometry of solutions and nitric acid concentration on wulfenite morphology. Table 1 is the extended and rearranged table of V e s s e l i n o v (1977) showing the conditions in 17 systematic experiments designed to study also the effect of supersaturation on growth morphology. It may be seen that from the left to the right in each row (e. g. from No 1 to No 6) the overall supersaturation decreased due to the decreasing concentrations of reactants (the law of mass action); it also decreased from the top to the bottom of each column (e. g. Nos 3, 8, 12, and 15) due to the increasing nitric acid concentration which raises lead molybdate solubility (G m e l i n, 1976). In exp. No 16, the metastable region of solubility was reached and no crystals formed. To grow them under those conditions (exp. No 17) crystal seeds were obtained under the conditions of exp. No 15, then they were allowed to grow under the conditions of exp. No 16. All experiments in Table 1 lasted about 20 days on the average and the crystals grew not larger than 0,3 mm. No effect of the decreasing supersaturation was observed except that the total mass of crystalline deposit diminished. The failure to observe anticipated morphological changes with supersaturation (К о с т о в,

Таблица 1

Условия в опитите с кристализационната апаратура. Разтвори на реагентите Pb^{2+} и MoO_4^{2-} постъпват непрекъснато, но без разбъркване в кристализационната колонка, като отношението на концентрациите им е 1:1 (фиг. 2). Всички разтвори съдържат и 0,06 mol/l NH_4NO_3; киселинността им е мерена с pH-метър (±0,02). Вътре в таблицата са дадени номерата на опитите

Table 1

Experimental conditions in the continuous-flow growth system. Reagent solution of Pb^{2+} and MoO_4^{2-} entered the crystallization column without stirring in a 1:1 concentration ratio (Fig. 2). All solutions contained 0,06 mol/l NH_4NO_3; their acidity was measured by a pH-meter (±0,02). Inside the table the experiments are consecutively numbered

HNO_3, mol/l	pH	Reagents, 10^{-4} mol/l				
		5	3	2	1	0,6
0,01	1,82	—	1,2	3	4	5,6
0,02	1,62	7	—	8	9	10
0,03	1,47	11	—	12	—	—
0,04	1,35	13	14	15	16,17	—

1973) was due to the two solution chemistry effects, so overwhelmingly pronounced that no other morphology vs. environment relations could be followed up in that experimental series. A summary of the observations is given in Fig. 2 which combines and extends the figures in Vesselinov, 1980, and Веселинов, 1992.

The top part of Fig. 2 shows the site of mixing and crystallization in the continuous-flow system (Vesselinov, 1976a). Lead nitrate (from the left), pure solvent (from above) and sodium or ammonium molybdate (from the right) entered the crystallization column at a rate of about 1 ml/hour and the reactants mixed together in a 1:1 concentration ratio without stirring (Table 1). The product of reaction, wulfenite, deposited as fine, clear crystals on pieces of plastic about 8 mm across, mounted perpendicular to the oncoming flow. Without the use of a stirrer, mixing of reactants across the crystallization column was poor (Vesselinov, 1976a), leading to concentration gradients of the reactants, the lead one diminishing to the right and the molybdate concentration dropping to the left. Nevertheless, the amount of deposit across the plastic substrates in any single experiment did not change appreciably (Pl. I, *1*) indicating that the overall supersaturation was approximately uniform across the column. Not so with the crystal forms. In every case without exception the crystals covering the plastic pieces on the lead side were dipyramids, whereas those on the molybdate side were platelets, and the two zones were distinctly divided by a narrow stripe of dipyramidal crystals with smaller or larger pinacoids (Pl. I, *1-4*). The growing acidity (Table 1) did not change in any way this separation of habits. Its powerful effect consisted in the appearance and increasing prominence of a steep dipyramid in general position {hkl} on the growth form (to be described in detail in the next section) with the increasing nitric acid concentration. Low-acid forms (0,01 and 0,02 mol/l HNO_3, Table 1) showed only {112} which on the higher-acid forms (0,03 and 0,04 mol/l HNO_3, Table 1) was gradually replaced by that steep dipyramid of convex but smooth faces (Pl. II, *1*, *2*).

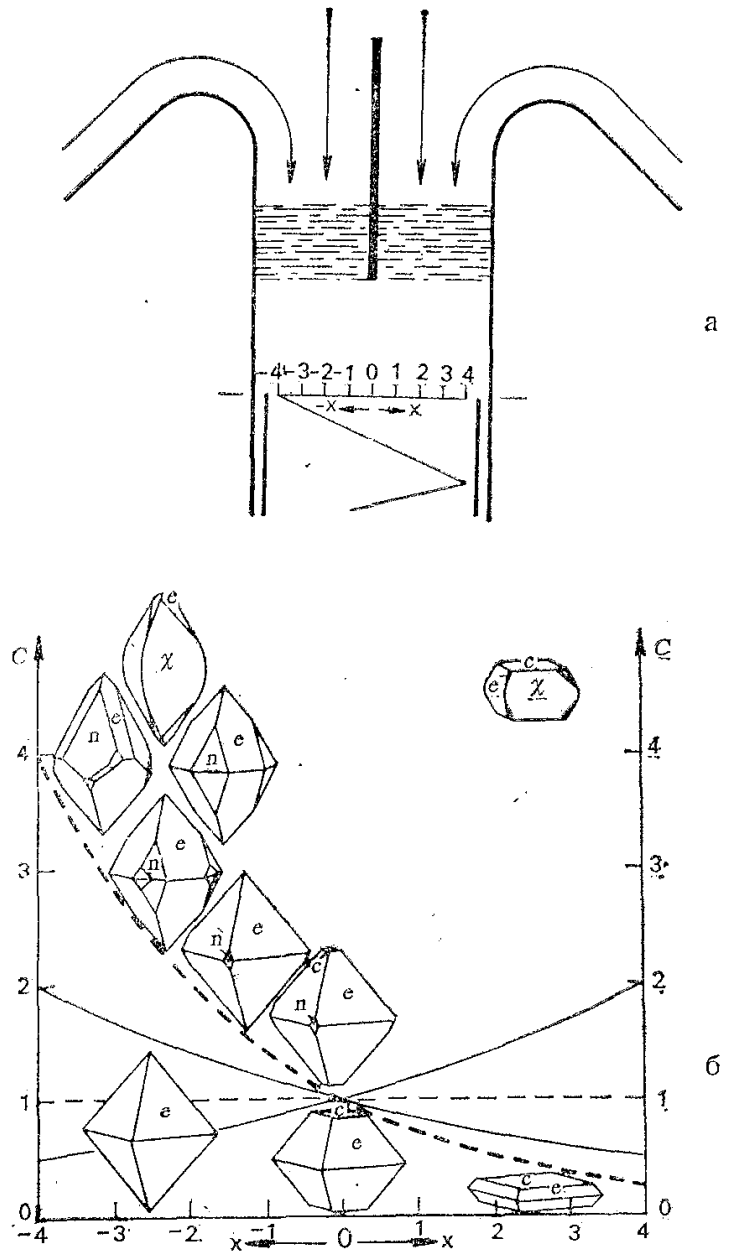

Fig. 2. Experimental set-up (above) and observed morphologies as dependent on the lead-to-molybdate ratio and the nitric acid concentration in solutions (see also Table 1 and text)
Фиг. 2. Схема на опитната постановка (горе) и получените форми в зависимост от оловно-молибдатното отношение и от концентрацията на азотната киселина в разтворите (вж. също Табл. 1 и текста)

All these relationships are schematically depicted in the lower diagram in Fig. 2. Its abscissa, x, runs along the diameter of the crystallization column with the origin in its centre as shown in the top part of the figure; the scale is in mm. The ordinates show the concentrations of reactants in arbitrary units. Solid lines represent the concentration variations across the site of crystallization, the lead concentration dropping to the right and that of molybdate to the left. These are idealized curves chosen to obey the laws $C_{Pb}=a^{-x}$ and $C_{MoO_4}=a^{x}$, where a is an arbitrary constant. Their product $C_{Pb}.\ C_{MoO_4}=1$,

shown by a dashed line, gives an idea of the uniform supersaturation across the site of crystallization. The other dashed curve is the ratio $C_{Pb}:C_{MoO_4}=a^{-2x}$ diminishing from the left to the right. The observed morphologies are arranged as dependent on that ratio and on the nitric acid concentration. The lower row shows the low-acid forms, and the upper row shows the high-acid ones with the steep convex dipyramid. In the left-handed half of the diagram, some measured dipyramidal crystals observed only in the gel experiments (V e s s e l i n o v, 1977) are added.

The above relations were tested in two separate experiments with 0,04 mol/l HNO_3 (cf. Table 1). In one of them 4.10^{-4} mol/l lead nitrate reacted with 1.10^{-4} mol/l sodium molybdate (lead-to-molybdate ratio 4:1) producing steep dipyramidal crystals only, with or without minor {112}. In the other, the ratio was inversed, 1:4, and all crystals developed somewhat curved pinacoids in addition to the former two forms. The high-acid habits, shown in Fig. 2, are measured crystals from these two experiments (see also Pl. II, *2*).

Morphological characterization

Many of the crystals, obtained by the author in the experiments of the foregoing section, were large enough (0,2÷0,5 mm) to permit measurements on a two-circle reflection goniometer; in difficult cases of curved and complex surfaces photogoniometry (V e s s e l i n o v, 1976b) was also used. Etching in 0,5% NaOH solution for 20 to 90 s was tried with some results but the small size of crystals precluded an extensive study. Scanning electron microscopy (JEOL Superprobe 733 and JSM 35) supplied decisive evidence supplementing the goniometric data. In one case the computer drawing procedure of V e s s e l i n o v (1994) by the program SHAPE was used to identify important morphological features on a SEM photograph. Below, the characteristics of the habit forms observed and their combinations are described.

The pinacoid *c* {001} shows the most variable surface relief ranging from perfectly flat and smooth (Pl. I, *3*, *4*), especially on the low-acid forms, to rounded (Pl. II, *3*) or very rough and irregular (Pl. II, *4*). Convex *c* surfaces, characterizing the high-acid forms, commonly have a flat central area and sloping sides producing crosslike reflection patterns rotated with respect to the crystal axes thus revealing the enantiomorphism of wulfenite. Etching for 30 s produces tetragonal etch pits on it (Pl. II, *7*, *8*) leaving *e* {112} unchanged. The pits are oriented parallel to the crystal axes as seen on the photographs. The crystal in Pl. II, *7* is oriented in such a way that its *a* and *b* axes, defined by the flat skeletal {112}, run parallel to the edges of the photograph, and the *c*-axis is perpendicular to it. The enlarged photo in Pl. II, *8* shows that the rectangular bases of the pits are also parallel to the edges of the photograph. Generally, *c* {001} can be described as the most morphologically unstable habit form in this study.

In contrast, *e* {112} is the most stable form showing practically always flat and smooth faces (Fig. 1; Pl. I, *2*, *3*; Pl. II, *1*, *5*, *7*). Measurements of their polar angles on 32 crystals gave a weighted mean of $\rho_{11\bar{2}}=57°39'\pm9'$, from which followed a mean morphological crystal-axes ratio of $c:a=2{,}233\pm0{,}013$. A very common feature of this form was the presence of one or two growth hillocks on some of its faces producing circular (from conical hillocks) or rounded-trigonal (from rounded pyramidal hillocks) reflections with diameters

ranging from one half to one and a half degrees of arc. These properties indicate a stable layer-by-layer mechanism of growth under the regimes in this study. *e* is most resistant to etching, too (Pl. II, *5, 7*).

The dipyramid *n* {011} is common on the gel-grown crystals (Fig. 1) and in some cases it becomes a habit form together with *e* (Fig. 2). Occasionally its faces are as flat as those of *e* but more often they are curved producing reflection patterns of one to three light rays extending close to [131], [111] or [151] (or [311], [111] and [511]) thus revealing the wulfenite hemihedry in the otherwise holohedral *n*+*e* combinations. In Fig. 2 a crystal of that type is depicted which also shows a kind of polar (hemimorphic, point group *4*) development with {011} larger than $\{01\bar{1}\}$ and {112} smaller than $\{11\bar{2}\}$. This is the only example of hemimorphism in the laboratory-grown crystals of this study although special efforts were made to find polar crystals. The etching behaviour of {011} could not be studied.

The high-acid habit form, the steep dipyramid {hkl} (Pl. I, *2. 3*; Pl. II, *1, 2*) was specially examined. Its faces, although convex, are as smooth as those of *e* even at high SEM magnifications showing no visible striations or sculpture of any sort. Six crystals (3 righthanded and 3 left-handed) were measured on the goniometer, in one of which the form was combined with *c* and *e*, and in the others with *e* only. Its faces produced scattered reflections extending over 50° of arc in meridional, and about 10° of arc in latitudinal direction. Although the patterns varied in the different crystals they generally obeyed the symmetry *4/m*. Fig. 3 is a projection on which all reflections observed from the six crystals are plotted to show that they are grouped around the poles of $\chi\{211\}$ and {121} somewhat closer to [110], $[1\bar{1}0]$ than to [100, [010]. This habit form reacts very characteristically to etching. After short exposures of 20÷30 s, leaving no traces on *e*, its faces decay into parallel ribs and grooves (Pl. II, *5*). To identify their directions, the SHAPE computer-drawing procedure of Vesselinov (1994) was used. The drawing in Pl. II, *6*, reproducing the etched crystal in Pl. II, *5*, is a combination of {112}, {354} and {121}. The edges between their faces are parallel to [131], $[\bar{3}11]$, and are also parallel to the etch ribs. This result supports the goniometric data (Fig. 3) showing that between {112} and {121} (or {211}) the face curvature follows the zones [131] (or [311]). To account for the properties of this rather unusual habit form, a bracketed symbol (χ) ({211}) or ({121}) was suggested (Веселинов, 1992) indicating its convex nature and its location near the form of planar faces and simple indices χ.

Summarizing the morphological evidence gained from the laboratory-grown wulfenite it should be noted that the anticipated genetic trend from tabular to steep dipyramidal habits with the increasing supersaturation (Костов, 1973, 1993) could not be tested. However, growth in acid solutions has revealed two powerful solution-chemistry effects on morphology (Fig. 2). It is also noteworthy that at pH below about 1,5 the face development of wulfenite drastically changes from holohedral *e* or *c*+*e* combinations of planar faces to hemihedral (χ) or *c*+(χ) ones of curved faces. To express this phenomenon in more definite morphological terms, the low-acid forms will be called "planihedra", and the high-acid ones "curvihedra".

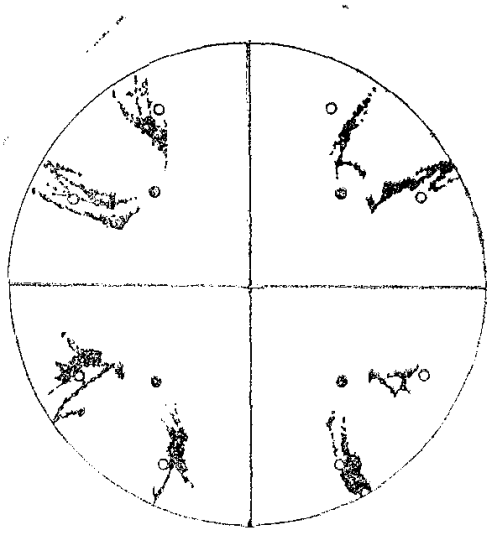

Fig. 3. The high-acid steep dipyramid (χ): combined projection of the reflection patterns from three right-handed and three left-handed habit curvihedra. Full circles {112}, open circles {211} and {121}
Фиг. 3. Стръмната бипирамида (χ), характерна за по-кисели разтвори: обща проекция на отраженията в гониометъра от три десни и три леви хабитусни кривостена. Черни кръгчета {112}, бели кръгчета {211} и {121}

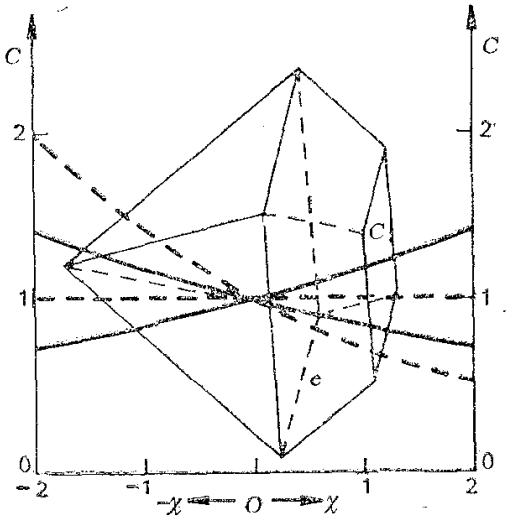

Fig. 4. Interpreting the wulfenite hemimorphism as a kinetically induced phenomenon obeying the law of Curie on the basis of the diagram in Fig. 2
Фиг. 4. Извеждане от фиг. 2 на хемиморфизма на вулфенита като явление, причинено от кинетични фактори при растежа му и контролирано от закона на Кюри

Discussion

The results of this study have a number of implications some of which will be discussed below with a view to future verification.

Firstly, the diagram in the lower part of Fig. 2. suggests an explanation of the morphological polarity, hemimorphism, of wulfenite as a growth phenomenon. Our hypothesis is illustrated in Fig. 4. It is the same crystallization site as in Fig. 2 with the lead-to-molybdate ratio gradient along the *x* axis. This time, however, a single crystal grows in it with its fourfold axis parallel to *x*. It is large enough to have one end in the excess-lead solution and the other in the excess-molybdate one. From our results it follows that the crystal will grow hemimorphic in such an environment. It may be seen also that this picture is derivable from the law of Curie. Indeed, the solution chemistry (the lead-to-molybdate ratio) of the growth environment in Fig. 4 has no mirror plane perpendicular to *x*. Then the law of Curie requires that the crystal will also lack a mirror plane perpendicular to its fourfold axis so that its symmetry will be reduced, *4* instead of *4/m*. Assuming that the same factor defines the morphology of natural wulfenite, the rarity of hemimorphic crystals can be ascribed to the small chances of suitably oriented specimens growing in high lead-to-molybdate ratio gradients commensurate with their size. However, if such specimens are found, for instance the type 2 crystals of D i e t r i c h (1972), their sharp pyramidal ends will point to the source of lead in the immediate environment as in Fig. 4. The absence of hemimorphism in

the other scheelite-type minerals is explained in this context with the absence of suitable cation-to-anion ratio gradients in their growth environments. The same reason would preclude hemimorphism in other crystals sensitive to that ratio (e. g. calcite, K i r o v et al., 1972).

Secondly, the observed specific crystal/solution interactions are consistent with the ideas of K l e b e r (1955/1956, 1956, 1957) who described the wulfenite hemimorphism as a typical case of hypomorphism, i. e. morphological symmetry lower than the true structural symmetry. In order to explain the feeble piezoelectric effect observed by H u r l b u t (1955) in natural crystals, that author (K l e b e r, 1956) suggested a structural reconstruction in the surface {001} layers based on the polarizability of lead ions and leading to slight distortions that would result in space group C_4^6-$I4_1$, indistinguishable by X-ray diffraction from C_{4h}^6-$I4_1/a$. Generally, K l e b e r (1955/1956, 1957) ascribed hypomorphism to the effect of selective adsorption on crystal faces during growth although in the case of wulfenite he emphasized lead polarizability. The results of this study, interpreted in terms of Kleber's views, provide clues that structural distortions may be related to adsorption (kinetic) effects and show a way of reconciling the mineralogical evidence for polar wulfenite with the laboratory evidence (e. g. G m e l i n, 1976) for centrosymmetric lead molybdate. A possible mechanism follows from certain well-known features of the structural and solution chemistry of molybdates and tungstates.

Our main argument is based on the similarities between the wolframite and scheelite types of ABO_4 structures discussed in detail by Д е м ь я н е ц et al. (1967). Divalent cations of radii smaller than about 1 Å, such as Fe, Mn, Zn, Cu, etc., form molybdates and tungstates of wolframite structure in which both the di- and hexavalent metals are coordinated to 6 oxygens, i. e. they consist of AO_6 and BO_6 octahedra. Divalent cations of larger radii, such as Ca, Sr, Ba and Pb, crystallize in scheelite structures characterized by AO_8 trigondodecahedra and BO_4 tetrahedra. As shown by these and other authors (e. g. S l e i g h t, 1972; H s u, 1981), the two structural types are closely related so that restricted solid solutions may be expected. The relevant fact here is that small displacements of the atoms in the AO_6/BO_6 wolframite arrangement are sufficient to reconstruct it into the AO_8/BO_4 scheelite structural type, as illustrated in Fig. 4 of Д е м ь я н е ц et al. (1967) (see also S l e i g h t, 1972). Following their scheme we have drawn Fig. 5 which shows a (220) structural slice of the wulfenite structure (according to the neutron-diffraction determination of Leciejewicz, 1965) in which the bottom $[\bar{1}10]$ structural chain consists of the scheelite-type PbO_8 and MoO_4 corner-sharing units whereas in the upper $[\bar{1}10]$ chain the bonding set is rearranged, without atomic displacements, into the wolframite-type corner-sharing octahedra. As for the displacements involved in such transformations, they can be illustrated with lead tungstate occurring both as stolzite, β-$PbWO_4$, which is a scheelite, and as raspite, α-$PbWO_4$, which is a wolframite (Д е м ь я н е ц et al., 1967). F u j i t a et al. (1977), who have determined the structure of raspite, comment that the volume difference between the two phases is only 0,53%, and the remarkable difference in coordination is the result of small displacements of the oxygens and relatively larger ones of the cations.

Another well known fact is that hexavalent molybdenum in solution is also coordinated to either four or six oxygens (G m e l i n, 1987, 1989; У э л л с, 1987). Monomer MoO_4 tetrahedra predominate at high pH and in

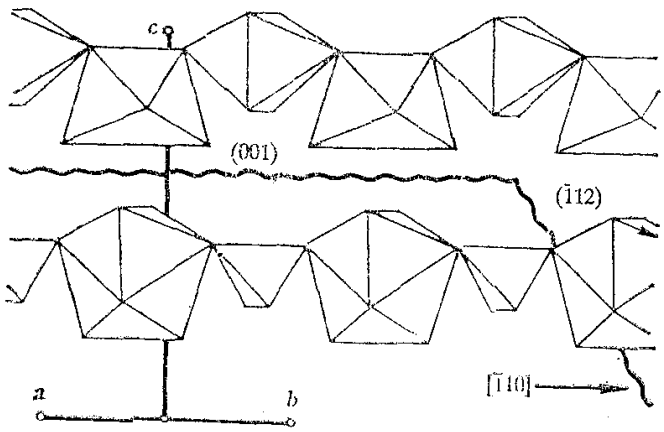

Fig. 5. A section of the wulfenite structure seen along [110] (the unit-cell edges are marked). The bottom [1̄10] chain consists of the scheelite-type PbO_8^{-}/MoO_4 polyhedra. In the upper chain the respective atoms are bonded in the wolframite-type pattern of cornre-sharing octahedra to illustrate the proposed mechanism of selective adsorption on {001} of either MoO_6 units or AO_6/MoO_6 ones (A=divalent metals of small radii such as Fe, Mn, Zn, etc.)

Фиг. 5. Част от структурата на вулфенита, гледана по [110] (отбелязана е елементарната клетка). Долната верига [1̄10] е изградена от шеелитовия тип полиедри PbO_8/MoO_4. В горната верига съответните атоми са свързани както във волфрамитовия тип структура (координационни октаедри с общи върхове), за да се покажат възможностите за избирателна адсорбция върху {001} на частици като MoO_6 или AO_6/MoO_6 (A=двувалентни метали с малки радиуси, напр. Fe, Mn, Zn и т. н.)

dilute solutions. With the growing acidity and concentration of solutions and in the presence of complexing agents, such as Si, P, etc., they polymerize into iso- and heteropolymolybdates built up of MoO_6 octahedra. These general features of the very complex structural (У э л л с, 1987) and solution (G m e l i n, 1987, 1989) chemistry of molybdates favour an assumption that the species responsible for the observed habit change in wulfenite should be sought among them. Let us consider the adsorption layer around a crystal growing in a solution of excess molybdate. Adsorption and long resident times of molybdate species on the available crystal surfaces would promote polymerization, i. e. surface formation of linked MoO_6 octahedra, even if the predominating species in solution are MoO_4 units. Structural considerations suggest that the {001} surfaces are best suited for stabilizing such polymers. Fig. 5 illustrates such a hypothetical situation of a chain of corner-sharing MoO_6 octahedra (a fragment of the MoO_3 structure, У э л л с, 1987) adsorbed on the (001) wulfenite layer. The rate of decomposition of such fragments into MoO_4 structural units will then become the rate-determining step in the (001) growth, retarding it relative to the supposedly less poisoned (112) layers. Selective adsorption and polymerization of molybdate ions on pinacoid surfaces would also favour the entrappment of smaller divalent ions, e. g. Zn, present in low concentration in the solution, to form wolframite-type $ZnO_6/$

MoO_6 chain fragments (Fig. 5) which, at higher growth rates, may be incorporated in the scheelite-type matrix, preferably in the {001} growth pyramids.

The inferred effect of selective adsorption is consistent with the observed characteristic morphological instability of wulfenite pinacoid surfaces as compared to the stable flat character of {112}. It is also consistent with the transference of yellow colour from silicomolybdate solutions to tabular crystals (Vesselinov, 1977) which besides that indicates that the wulfenite structure tolerates incorporation even of species as complex as heteropolymolybdates. Supporting evidence is also provided by some data on the morphology and the impurities in scheelites and wolframites. Костов (1961) described steep dipyramidal wulfenite growing over galena. In natural wulfenites, Кольковски, Брескovска (1965) and Kol'kovski, Breskovska (1968) reported increased amounts of Zn and Si in tabular crystals. Grubb (1967) described zoned ferberitic wolframite with scheelite exsolutions, and Hsu (1981) suggested an interpretation involving the formation of a metastable scheelite-wolframite solid solution during rapid growth with subsequent exsolution. It is clear that such a model requires CaO_6/WO_6 wolframite-type coordinations prior to the transformation to the CaO_8/WO_4 scheelite structure. In the same study, Hsu (1981) once again resorted to kinetic effects in an attempt to explain the formation of wolframite-type raspite in nature as contrasted to the failures of its laboratory synthesis which had yielded scheelite-type stolzite only. Finally, Жильцова et al. (1969), studying synthetic powellites, recorded MoO_6 lines in addition to the MoO_4 ones in their infra-red spectra and ascribed them to "deformed fragments" in the scheelite-type structure using arguments based on the analysis of Демьянец et al. (1967).

The occurrence of the enantiomorphic high-acid "curvihedron" (χ) as a habit form is also an interesting phenomenon. Firstly, structural analysis had shown (Vesselinov, 1971) that even the form of planar faces χ is of kinked character so that normally it could not be expected to develop as a habit form (Hartman in Sunagawa, 1987). Such habit forms in general position {hkl} are rare in mineral crystals: monohydrocalcite, described by Minčeva-Stefanova, Neykov (1990), is the only well documented example known to the author. Secondly, the form combines smoothness with convexity which is also rare. In natural wulfenites, steep curved dipyramids are known (e. g. Костов, 1993); Rothwell, Mason, 1991; Grafenauer, Mirtič, 1972) but correct identifications of their positions with respect to the crystal axes are lacking (for instance, Grafenauer, Mirtič, 1972, ascribed a symbol on the basis of polar angles only). This permits only a broad assumption that at least some of them correspond to the curvihedron observed on our crystals. If that is so, a mechanism of their formation will have to account for a wider range of environments than the laboratory ones, including for instance solutions of high pH values. It is also clear that such a mechanism should differ from the one responsible for the habit change because their morphological effects occur independently of each other.

Recent work on crystal morphology (Sunagawa, 1987) has shown that a problem of this kind can be approached by considering the R, θ plots of crystal surfaces, i. e. diagrams in which the growth rates R along the normals to the surface are plotted as a function of the orientation angle θ similarly to Wulf plots of the surface free energy vs. orientation used for equilibrium forms. Fig. 6 represents the observed high-acid growth morphology in terms of an R, θ plot in the zone $[\bar{3}11]$ where the habit curvihedron (χ) is combined

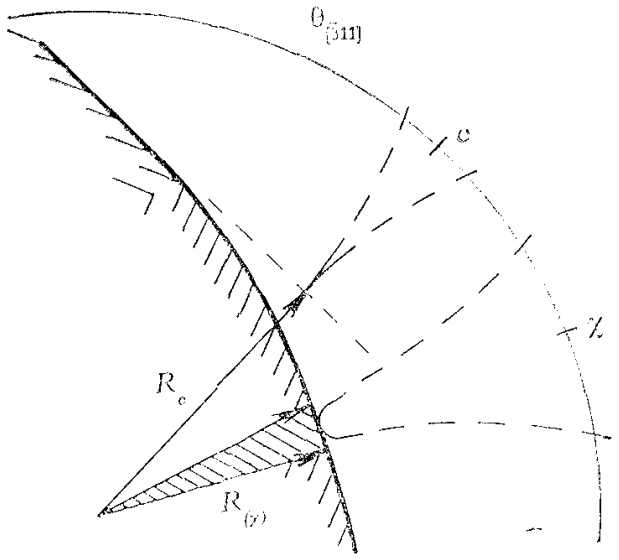

Fig. 6. Growth rate (R) vs. orientation (θ) plot (dashed line) in the [$\bar{3}$11] zone derived from the observed high-acid morphology to interpret its growth mechanism. The poles of *e* and χ are marked on the zone circle (thin line). The crystal surface (hatched) consists of planar *e* and curved (χ) areas (thick line) defining on the plot a sharp singular cusp and a rounded cusp, respectively

Фиг. 6. Диаграма на скоростите на растеж (R) в зависимост от ориентацията (θ) (щрихова линия) в зоната [$\bar{3}$11], изведена от формите на растеж в по-кисела среда за тълкуване на механизма на образуването им. Върху зоналния кръг са отбелязани полюсите на *e* и χ. Кристалната повърхност (щрихована) се състои от плоски *e* и криви (χ) области (плътна линия), които върху диаграмата определят съответно един остър сингуларен минимум и един заоблен минимум

with the minor planihedron *e*. In accord with the morphological evidence, the layer growth of the flat *e* at a rate R_e defines a sharp cusp on the plot. The area around χ (121) is curved, so that it must be defined by a rounded cusp corresponding to a range of $R_{(\chi)}$ values inside some restricted angle θ (their small local variations explain the variable curvature of the faces of the otherwise stationary curvihedron). Such surfaces (H a r t m a n and S u n a g a w a in S u n a g a w a, 1987) are of kinked character, i. e. they are rough on an atomic scale, and grow continuously normal to themselves because growth sites are available everywhere on the surface. Due to this low resistance to growth they normally do not appear on the growth form. It has been shown (B e n n e m a, van der E e r d e n and H a r t m a n in S u n a g a w a, 1987) that interaction of such surfaces with the motherphase may cause them to develop on the crystal. K e r n (in S u n a g a w a, 1987) has demonstrated that on equilibrium forms curved areas also develop as a result of preferential adsorption in the kinks.

Thus, recent studies suggest again an adsorption mechanism for the enantiomorphic curvihedron. Now we need to answer the question which structural

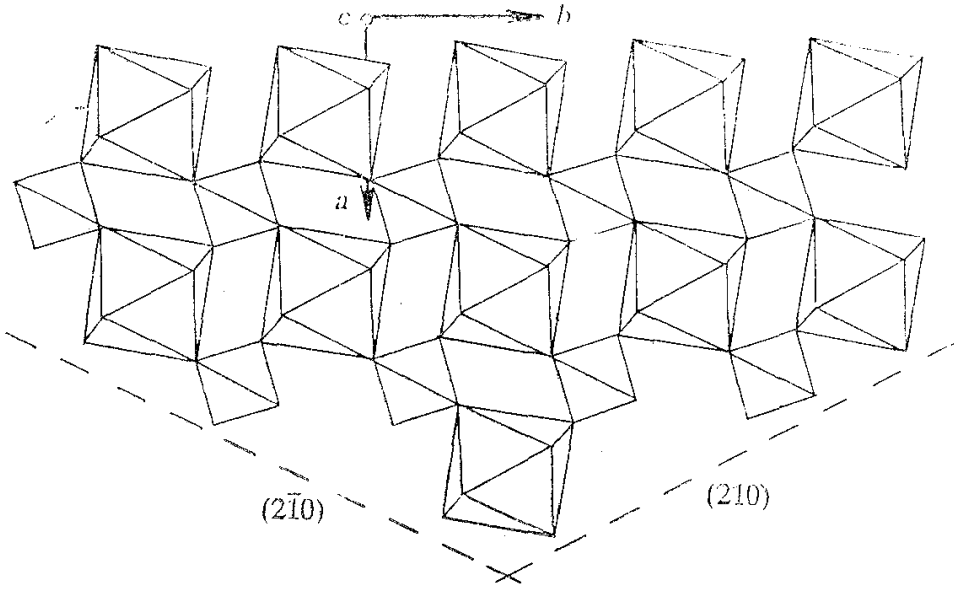

Fig. 7. A 004 slice of the wulfenite structure seen along [001] and represented by PbO_8 /MoO_4 coordination polyhedra (the unit cell is marked). Note the geometrical difference between the two kinds of kinks along the hemihedral planes (2$\bar{1}$0) and (210) shown by dashed lines
Фиг. 7. Проекция по [001] на един слой 004 на структурата на вулфенита, представена с координационни полиедри PbO_8 /MoO_4 (отбелязана е елементарната клетка). Двете структурни стъпала по хемиедричните равнини (2$\bar{1}$0) и (210) (щрихови линии) се различават по геометрията си

surfaces provide the adsorption sites. Evidently, they must be related to the oxygen framework of the structure since it is the carrier of énantiomorphism in wulfenite (L e c i e j e w i c z, 1965). The problem we are faced with is exemplified by Fig. 7 which shows a (004) slice of the wulfenite structure seen along [001]. The pattern of PbO_8 and MoO_4 structural units cut along (2$\bar{1}$0) and (210) defines two kinds of kinks which may serve as adsorption sites in a situation similar to that under discussion. Geometrically, the difference between them is rather small which suggests that special efforts will be needed to identify the chemical species responsible for the formation of the curvihedron. The results of this study are insufficient to allow further inquiry into this problem.

Conclusion

The two powerful solution-chemistry effects on wulfenite morphology described here present new opportunities for gaining knowledge about processes taking place on the crystal /solution interface during growth. A number of implications have remained unexplored in our analysis made rather to outline the need of future work on artificial and natural material. The proposed mechanisms of selective adsorption are general enough to expect similar effects in other related minerals. In wulfenite in particular it seems probable that phenomena induced by growth kinetics may be responsible both for its morphological and structural polarity which suggests that wulfenite piezoproperties, so far observed in natural crystals only, could be reproduced and even amplified in the laboratory.

The author is indebted to his late colleague O. Dimitrov, and to Ts. Iliev and E. Mandova at the Geological Institute for the SEM photographs. Part of this study was supported by the National Scientific Fund, Grant No 2/91.

References

Веселинов, И. 1992. Кристална морфология и условия на минералообразуване — примери от кристализацията на вулфенита. — В: Сб. рез. „Постижения и задачи на българската минералогия и петрология", Научна сесия, С., 10—11.

Демьянец, Л. Н., В. В. Илюхин, А. В. Чичагов, Н. В. Белов. 1967. О кристаллохимии изоморфных замещений в молибдатах и вольфраматах двухвалентных металлов. — Изв. АН СССР, Неорг. матер., **3**, № 12, 2221—2234.

Жильцова, И. Г., Л. Н. Карпова, Г. А. Сидоренко, А. А. Валуева, А. Д. Дара. 1969. О низкотемпературных синтезах повеллита. — Геохимия, **2**, 147—156.

Кольковски, Б., В. Бресковска. 1965. Парагенеза и кристаломорфология на вулфенита от Родопските оловно-цинкови месторождения. — Год. СУ, Геол.-геогр. фак., **58**, кн. 1 — Геология, 117—133.

Костов, И. 1961. Принос към морфологията на вулфенита. — Тр. геол. България, сер. геохим. и пол. изк., II, 121—129.

Костов, И. 1962. Генетические типы габитусов минералов. — Мин. сб. Львов, **16**, 75—90.

Костов, И. 1973. Минералогия (III изд.). С., Наука и изкуство. 674 с.

Костов, И. 1993. Минералогия (IV изд.). С., Техника. 734 с.

Уэллс, А. 1987. Структурная неорганическая химия, т. 2. М., Мир. 694 с.

Dietrich, J.-E. 1972. La wulfénite de la mine de Bou-Skour, quartier de la Patte d'Oie (Jbel Sarhro, Maroc). — Notés Serv. géol. Maroc, **32**, No 241, 25-29.

Fujita, T., I. Kawada, K. Kato. 1977. Raspite from Broken Hill. — Acta Cryst., B**33**, 162-164.

Gmelin Handbuch der anorganischen Chemie, 1976. Bd. 53; Erg.-Bd. B2; 1987. Suppl. B3a; 1989. Suppl. B3b. Berlin-Heidelberg-New York, Springer Verlag.

Grafenauer, S., B. Mirtič. 1972. Unusual wulfenite crystals from Mežica. — Rud.-Met. Zb., **4**, 329-330.

Grubb, P. L. C. 1967. Solid solution relationships between wolframite and scheelite. — Amer. Mineral., **52**, 418-426.

Hanneberg, A. 1989. Ein bemerkenswerter Eigenfund — Wulfenit aus Tirol. — Lapis, **1**, p. 38.

Hsu, L. C. 1981. Phase relations of some tungstate minerals under hydrothermal conditions. — Amer. Mineral., **66**, 298-308.

Hurlbut, C. S. 1955. Wulfenite symmetry as shown on crystals from Jugoslavia. — Amer. Mineral., **40**, 857-860.

Kirov, G. K. 1972. On the diffusion method for growing crystals. — J. Cr. Growth, **15**, No 2, 102-106.

Kirov, G. K., I. Vesselinov, Z. Cherneva. 1972. Conditions of formation of calcite crystals of tabular and acute rhombohedral habits. — Krist. Techn., 7, No 5, 497-509.

Kleber, W. 1955/1956. Über Hypomorphie. — Wiss. Z. Humboldt-Univ. Berlin, Mathem.-Naturwiss. Reihe, **5**, No 1, 1-13.

Kleber, W. 1956. Zum Problem der polaren Hemiedrie (Ein Beitrag zur Symmetrie des Wulfenits). — Chemie der Erde, **18**, No 3, 167-178.

Kleber, W. 1957. Hypomorphie und morphologischer Aspekt. — N. Jb. Miner., Mh., **5**, 105-112.

Kol'kovski, B., V. Breskovska. 1968. Zur Mineralparagenese des Wulfenits. — Freiberger Forschungsh., C-230 — Mineralogie-Lagerstättenlehre, 377-385.

Kostov, I. 1965. Crystal habit and mineral genesis. — Bull. Inst. Geol., **14**, 33-49.

Leciejewicz, J. 1965. A neutron crystallographic investigation of lead molybdenum oxide, $PbMoO_4$. — Z. Krist., **121**, 158-164.

Minčeva-Stefanova, J., H. Neykov, 1990. Trigonal-trapezohedral monohydrocalcite from an oxidation zone. — C. R. Acad. bulg. Sci., **43**, No 2, 57-60.

Mineralogical Record. 1990. **21**, No 1-2, 99-100.

Pillai, K. S., M. A. Ittyachen. 1977a. Observations on the growth of single crystals of lead molybdate from gels. — J. Cr. Growth, **39**, No 2, 287-290.

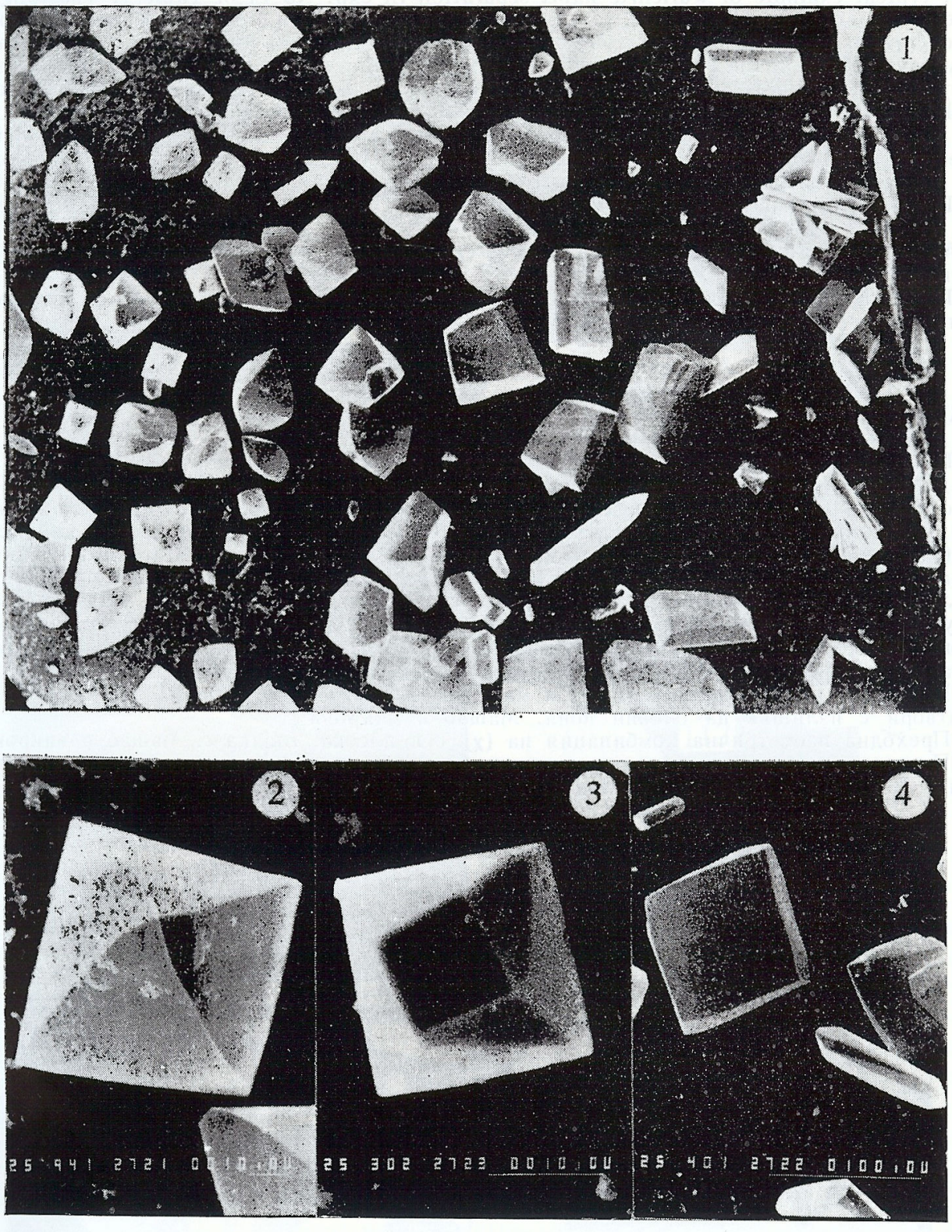

Геохимия. минералогия и петрология, кн. 30, И. Веселинов — Krnetically induced morphological . . .

PLATE I

1. A typical example of wulfenite habit separation in exp. No 14 of Table 1. The longer edge of the SEM photo is parallel to *x* in Fig. 2 and is about 1 mm long. The mass of deposited crystals is uniformly distributed over the substrate. Dipyramidal $e+(\chi)$ crystals only have grown on the excess-lead side (left) and tabular $c+(\chi)+e$ ones cover the excess-molybdate side (right). The two areas are divided by a distinct band of intermediate morphologies, the pinacoid showing skeletal development. The crystal indicated by the arrow has its fourfold axis parallel to *x* and has developed a small *c* surface on the molybdate side only (compare with Fig. 4). Wulfenite habits from the same experiment, seen along the fourfold axis, are illustrated below
2. The high-acid excess-lead combination of the curvihedron (χ) with the minor planihedron *e*. Scale bar in microns
3. An intermediate isometric combination of (χ), *e* and flat and smooth *c*. Scale bar in microns
4. The high-acid excess-molybdate tabular combination with flat and smooth *c*. Scale bar in microns

ТАБЛО I

1. Типичен случай на разделяне на хабитусите на вулфенита в опит № 14 от Табл. 1. По-дългата страна на СЕМ снимката е успоредна на *x* от фиг. 2 и е около 1 мм. Масата от отложени кристали е разпределена равномерно върху подложката. Само бипирамидални кристали $e+(\chi)$ са расли откъм излишъка на олово (отляво), а плочестите кристали $c+(\chi)+e$ покриват подложката откъм излишъка на молибдатни йони (отдясно). Двете области са разделени от ясна ивица с преходни форми, върху които пинакоидът показва скелетно развитие. Кристалът, посочен със стрелката, е разположен с четворната си ос успоредно на *x* и е развил малка повърхност *c* само откъм молибдатната страна (срв. с фиг. 4). Долу са илюстрирани вулфенитови форми от същия опит, гледани по четворната ос
2. Комбинацията от кривостена (χ) и малък плоскостен *e*, характерна за по-киселите разтвори с излишък на оловни йони. Мащаб в микрони
3. Преходна изометрична комбинация на (χ), *e* и плоска, гладка *c*. Мащаб в микрони
4. Плочеста комбинация, характерна за по-киселите разтвори с излишък на молибдатни йони. В случая *c* е плоска и гладка. Мащаб в микрони

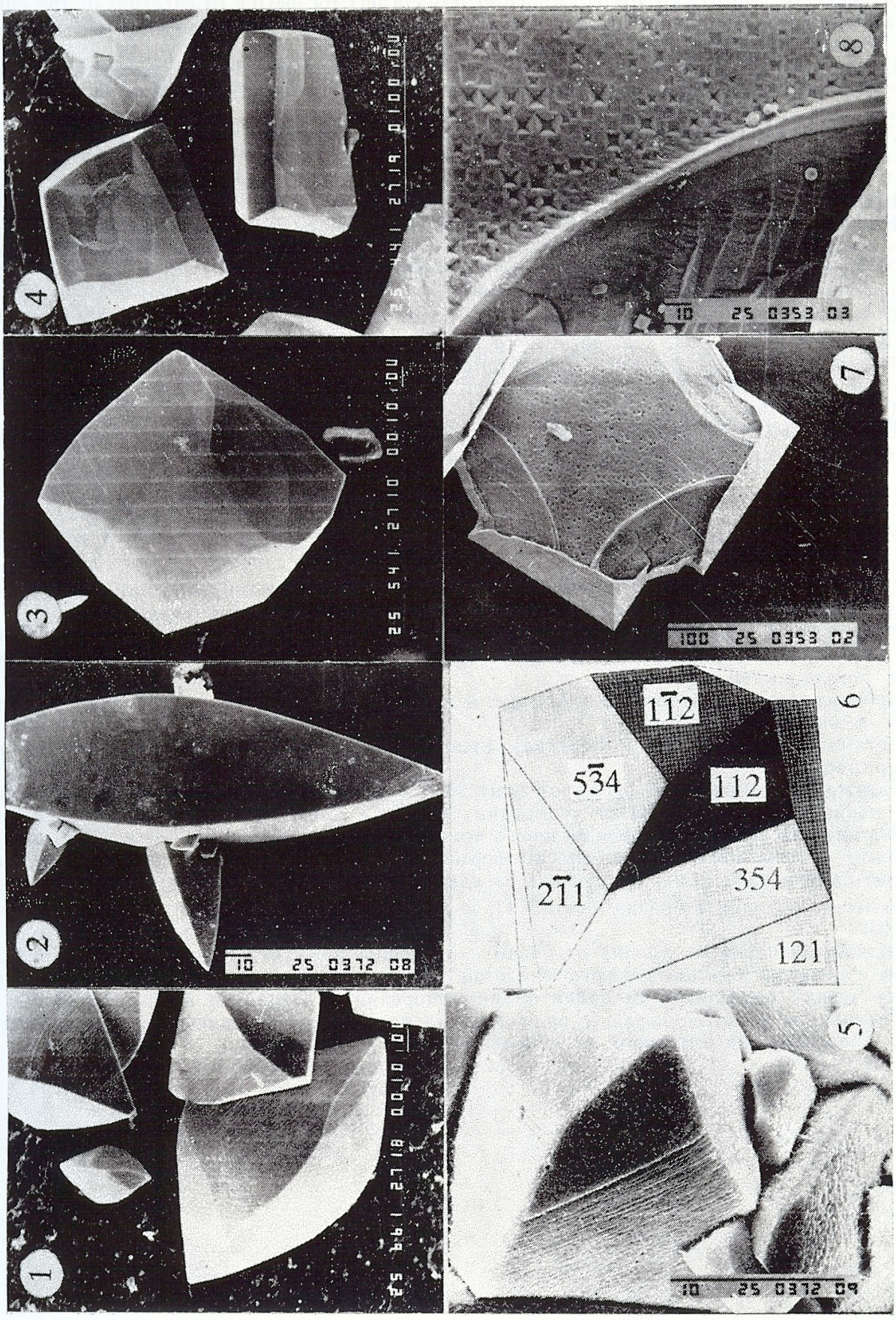
1
2
3
4
5
6
7
8
$1\bar{1}2$
$5\bar{3}4$
112
$2\bar{1}1$
354
121

PLATE II

1. A detail of photo *1* in Plate I (bottom left corner) for better illustration of the curved character of (χ) as compared to the planar *e* and the equal smoothness of their faces. Scale bar in microns
2. Crystals from the test experiment with a 4:1 lead-to-molybdate concentration ratio. They are dominated by the curvihedron (χ) characterized by the absence of any surface relief
3. A thick-tabular excess-molybdate combination from exp. No 11, Table 1, with rounded *c* and planar *e*
4. A detail of photo *1* in Plate I (centre) showing tabular crystals with very irregular *c* surfaces
5. Etched (χ)+*e* combination from exp. 13, Table 1. The curvihedral surfaces have decayed into systems of parallel grooves whereas the planihedral ones have remained undamaged
6. A SHAPE computer-drawing reproduction of the form in *5.* on which the curvihedron is represented by the two planar forms {121} and {354}. The angles between the respective edges of the crystal and of the drawing are equal which permits to identify the directions of the etch ribs as [$\bar{3}$11], i. e. parallel to the edges between {121}, {354} and {112}
7. An etched skeletal platelet from counterdiffusion experiments in free of gel systems. The *c* surface is covered with etch pits whereas the *e* faces have remained undamaged. Note that the edges between the latter are nearly parallel to the edges of the photo
8. Enlarged detail of photo *7.* to show the shape of the etch pits and their parallel orientation with respect to the edges of the photograph

ТАБЛО II

1. Детайл от сн. *1.* Табло I (долния ляв ъгъл), за да се види по-добре кривата (χ) наред с плоската *e* и това, че стените им са еднакво гладки. Мащаб в микрони
2. Кристали от пробния опит с оловно-молибдатно отношение на концентрациите 4:1. За тях е типичен кривостенът (χ), чийто стени се характеризират с липса на какъвто и да е повърхностен релеф
3. Дебелоплочеста комбинация с крива *c* и плоска *e* от зоната с излишък на молибдатни йони в опит № 11, Табл. 1
4. Детайл от сн. *1*, Табло I (центъра), където плочестите кристали са с много неравни повърхности *c*
5. Разяждана комбинация (χ)+*e* от опит № 13, Табл. 1. Повърхността на кривостена се е разпаднала на система от успоредни бразди, а плоскостенът е останал незасегнат
6. Формата на сн. *5*, е възпроизведена с компютърен чертеж с програмата SHAPE. Кривостенът е представен с двете плоски форми {121} и {354}. Ъглите между съответните ръбове на кристала и върху чертежа са еднакви, което позволява да се идентифицират посоките на разядните бразди като [$\bar{3}$11], т. е. успоредни на ръбовете между {121}, {354} и {112}
7. Разяждана скелетна плочка от опити с насрещна дифузия. Повърхността на *c* е покрита с разядни ямички, докато стените на *e* са останали незасегнати. На снимката ръбовете между последните са ориентирани успоредно на страните на снимката
8. Увеличение на сн. *7*, за да се види формата на разядните ямички и тяхната ориентация, успоредна на страните на снимката

Pillai, K. S., M. A. Ittyachen. 1977b. Habit modifications in lead molybdate crystals grown in gels. — Indian J. Pure Appl. Phys., **15**, No 3, 204-206.
Rothwell, M., J. Mason. 1991. Wulfenite in the British Isles. — UK J. Mines Miner., **11**, 30-41.
Sleight, A. W. 1972. Accurate cell dimensions for ABO_4 molybdates and tungstates, — Acta Cryst., B28, 2899-2902.
Sunagawa, I. (Ed.). 1987. Morphology of Crystals, Parts A and B, Tokyo, Terrapub. 741 p.
Vesselinov, I. 1971. Relation between the structure of wulfenite, $PbMoO_4$, as an example of the scheelite type of structure, and the morphology of its crystals. — J. Cr. Growth, **10**, No 1, 45-55.
Vesselinov, I. 1976a. Experimental arrangement for growing crystals of sparingly soluble compounds under ambient conditions. — C. R. Acad. bulg. Sci., **29**, No 6, 857-860.
Vesselinov, I. 1976b. On the photogoniometric method of examining crystals with complex surfaces, Parts I and II. — Krist. Techn., **11**, No 1, 23-30, 31-40.
Vesselinov, I. 1977. On the yellow colour of wulfenite ($PbMoO_4$) crystals. — Krist. Techn., **12**, No 5, K36-K38.
Vesselinov, I. 1980. Solution growth of wulfenite crystals and their morphology as related to the growth conditions. — Ext. Abstr. 6th Intern. Conf. Cr. Growth, Moscow, **IV**, 198-199.
Vesselinov, I. 1994. The SHAPE crystal-drawing computer program as an instrument in research. — Geochem., Mineral. and Petrol., **29**, 97-105.
Zirkl, E. J. 1988. Bleiberg-Kreuth, die berühmte Wulfenit-Fundstelle in Kärnten. — Lapis, **78**, 1965.

Одобрена на 9. VI. 1994 г. *Accepted June 9, 1994*